



## Structure and properties of $(25 - x/2)\text{Li}_2\text{O} \cdot (25 - x/2)\text{Na}_2\text{O} \cdot x\text{PbO} \cdot 50\text{P}_2\text{O}_5$ metaphosphate glasses

Francisco Muñoz <sup>a,\*</sup>, Fernando Agulló-Rueda <sup>b</sup>, Lionel Montagne <sup>c</sup>,  
Roger Marchand <sup>d</sup>, Alicia Durán <sup>a</sup>, Luis Pascual <sup>a</sup>

<sup>a</sup> Instituto de Cerámica y Vidrio, Consejo Superior de Investigaciones Científicas (CSIC), Cl Kelsen s/n, Cantoblanco, 28049 Madrid, Spain

<sup>b</sup> Instituto de Ciencia de Materiales de Madrid (CSIC), Cantoblanco, 28049 Madrid, Spain

<sup>c</sup> Laboratoire de Cristallogénie et Physicochimie du Solide, ENSCL, 59655 Villeneuve d'Ascq, France

<sup>d</sup> Laboratoire Verres et Céramiques, UMR CNRS 6512, Institut de Chimie, Université de Rennes I, 35042 Rennes cedex, France

Received 5 March 2004; received in revised form 15 June 2004

### 12 Abstract

13 The structure of  $(25 - x/2)\text{Li}_2\text{O} \cdot (25 - x/2)\text{Na}_2\text{O} \cdot x\text{PbO} \cdot 50\text{P}_2\text{O}_5$  phosphate glasses ( $0 \leq x \leq 50\text{mol}\%$ ) has been investigated by  
14 Raman spectroscopy, and  $^{31}\text{P}$ -MAS and  $^{207}\text{Pb}$ -VOCS nuclear magnetic resonance. An increase in lead content affects the  $\text{PO}_4$  tetra-  
15 hedra network by weakening bonds between phosphorus and non-bridging oxygens. At low concentration, lead behaves as a mod-  
16 ifier cation, with large coordination number. For higher PbO contents, a decrease in the coordination number of the  $\text{Pb}^{2+}$  cations  
17 and an increase in the covalent character of the Pb–O bonds is observed. The changes in density and thermal properties of the glasses  
18 are explained through the structural evolution. The non-linear increase of the glass transition and dilatometric softening tempera-  
19 tures with PbO content is related to the non-linear variation of the PbO molar volume. This behavior is discussed in terms of the  
20 change in lead coordination when PbO is introduced in a mixed-alkali metaphosphate glass composition.

21 © 2004 Published by Elsevier B.V.

### 23 1. Introduction

24 Phosphate glasses have specific properties such as low  
25 glass transition ( $T_g$ ) and dilatometric softening ( $T_s$ ) tem-  
26 peratures, high coefficients of thermal expansion (CTE)  
27 or high UV transparency. These properties make them  
28 interesting materials for applications in low-temperature  
29 sealing [1–6], vitrification of nuclear wastes [7,8], as well  
30 as laser host matrices after doping with rare-earth ele-  
31 ments [9–12]. The low durability of phosphate glasses  
32 can be improved by the substitution of nitrogen for oxy-  
33 gen, which leads to a higher cross-linking density of the

glass network [13,14]. Most of the studies reported on  
phosphate oxynitride glasses have dealt with alkali  
phosphates (Na,Li) [15,16], mostly because the nitrida-  
tion under ammonia atmosphere must be carried out  
at low temperature in order to avoid reduction reac-  
tions. However, we have been able to prepare lead oxy-  
nitride phosphate glasses [17], because lead can be  
introduced in phosphate glasses without increasing the  
temperature at which the melt viscosity is low enough  
to enable nitridation.

Indeed, the high ionic field strength (IFS) and polar-  
izability of  $\text{Pb}^{2+}$  cations give lead phosphate glasses low  
 $T_s$  as well as high CTE values and a relatively high  
chemical durability. Moreover, lead can be incorporated  
in a phosphate glass network up to proportions as large  
as 66mol%, consequently lead phosphate glasses have  
been widely studied as low-temperature sealing materi-

\* Corresponding author. Present address: Laboratoire Verres et  
Céramiques, UMR CNRS 6512, Institut de Chimie, Université de  
Rennes I, 35042 Rennes cedex, France. Tel.: +33 223 23 62 64/34 91  
735 58 40x1233; fax: +33 223 23 59 59/34 91 735 58 43.

E-mail address: [fmunoz@icv.csic.es](mailto:fmunoz@icv.csic.es) (F. Muñoz).

Table 1

Nominal and analyzed  $(25 - x/2)\text{Li}_2\text{O} \cdot (25 - x/2)\text{Na}_2\text{O} \cdot x\text{PbO} \cdot 50\text{P}_2\text{O}_5$  glass compositions

Mol% PbO	Li <sub>2</sub> O nominal	Li <sub>2</sub> O analyzed (±0.1%)	Na <sub>2</sub> O nominal	Na <sub>2</sub> O analyzed (±0.1%)	PbO nominal	PbO analyzed (±0.2%)	P <sub>2</sub> O <sub>5</sub> nominal	P <sub>2</sub> O <sub>5</sub> analyzed (±0.5%)
0	25	22.7	25	25.3	–	–	50	51.9
10	20	17.8	20	20.3	10	9.9	50	52
20	15	13.6	15	15.6	20	20.6	50	50.1
25	12.5	10.5	12.5	12.2	25	26.1	50	51.2
30	10	9.3	10	10.6	30	31	50	49.1
40	5	4.5	5	5.3	40	40.2	50	49.9
50	–	–	–	–	50	50.2	50	49.8

51 als [5]. Depending on the studied system, the  $\text{Pb}^{2+}$  ions  
52 show an intermediate character between former and  
53 modifier. While in silicate glasses the coordination num-  
54 ber is between 2 and 4, and lead behaves as an interme-  
55 diate element [18], in phosphate glasses the lead cations  
56 are assumed to play a modifier role with higher coordi-  
57 nation numbers [19,20].

58 The present work is part of a study mainly devoted to  
59 phosphorus oxynitride glasses. Such glass compositions  
60 result from a progressive nitrogen/oxygen substitution  
61 within the phosphate glass network, with formation of  
62 P–N bonds at the expense of P–O bonds when an oxide  
63 glass precursor is melted in flowing ammonia. We have  
64 described previously the preparation conditions as well  
65 as the main characteristics of ‘LiNaPbPON’ glasses as  
66 a function of the nitrogen enrichment [17,21]. We have  
67 also performed a structural study of the  $\text{Li}_{0.25}\text{Na}_{0.25}$ -  
68  $\text{Pb}_{0.25}\text{PO}_{3-3x/2}\text{N}_x$  glass series ( $0 < x \leq 0.69$ ), and the  
69 structural role of lead has been interpreted from a com-  
70 parison with similar ‘LiNaPON’ glasses [22]. It has been  
71 shown that the presence of  $\text{Pb}^{2+}$  ions affects the nitrida-  
72 tion mechanism, and, moreover, that their network for-  
73 mer character increases with nitridation [21]. The role of  
74 lead in oxide phosphate glasses has been studied in  
75 many phosphate glass compositions [23–25], however,  
76 we could not find any data on the introduction of lead  
77 in a mixed Li–Na metaphosphate composition. The  
78 aim of the present study is thus an investigation of ‘LiN-  
79 aPb’ metaphosphate glasses. The effect of increasing  
80 amounts of lead is reported for  $(25 - x/2)\text{Li}_2\text{O} \cdot$   
81  $(25 - x/2)\text{Na}_2\text{O} \cdot x\text{PbO} \cdot 50\text{P}_2\text{O}_5$  glass compositions  
82 with  $0 \leq x \leq 50$  mol%. Structural data from Raman  
83 and nuclear magnetic resonance spectroscopies are gi-  
84 ven, and they are completed with density and thermal  
85 properties measurements.

## 86 2. Experimental

87 Metaphosphate glass compositions  $(25 - x/2)\text{Li}_2\text{O} \cdot$   
88  $(25 - x/2)\text{Na}_2\text{O} \cdot x\text{PbO} \cdot 50\text{P}_2\text{O}_5$  ( $0 \leq x \leq 50$  mol%)  
89 were prepared by melting reagent grade  $\text{Li}_2\text{CO}_3$ ,  
90  $\text{Na}_2\text{CO}_3$ ,  $\text{Pb}_3\text{O}_4$  and  $\text{H}_3\text{PO}_4$  (85 wt%,  $d = 1.7 \text{ g cm}^{-3}$ ) in  
91 a gas furnace. The batches were first calcined in porce-

92 lain crucibles up to 450 °C for a week, then melted at  
93 1100 °C for 1 h. The melts were poured on brass plates  
94 in air, then the glasses were annealed for 30 min at tem-  
95 peratures close to  $T_g$ . The glass samples were clear, col-  
96 orless, and bubble free.

97 The glass compositions were chemically analyzed by  
98 inductively coupled plasma-emission spectrometry  
99 (ICP) with a *Thermo Jarrel Ash IRIS ADVANTAGE*  
100 spectrometer, and flame photometry (FP) with a *Perkin*  
101 *Elmer 2100* spectrometer. The powdered glasses were  
102 dissolved in diluted hot hydrochloric acid. The PbO  
103 and  $\text{P}_2\text{O}_5$  contents were measured by ICP while alkali  
104 oxides were determined by FP. The nominal and exper-  
105 imental compositions of the glasses prepared are shown  
106 in Table 1.

107 The Raman spectra of the phosphate glasses were ob-  
108 tained with a *Renishaw Ramascope 2000* spectrometer.  
109 The calibration was made using the  $520.0 \text{ cm}^{-1}$  Raman  
110 peak of a Si(001) single crystal. An  $\text{Ar}^+$  laser at  
111 514.5 nm wavelength was used, with a 5 mW power  
112 and a spot diameter of 1  $\mu\text{m}$  on the sample. The spectral  
113 resolution and frequency accuracy were  $4 \text{ cm}^{-1}$  and  
114  $0.5 \text{ cm}^{-1}$ , respectively, and the acquisition time 100 s  
115 per point. The spectra were recorded at 300 K.

116  $^{31}\text{P}$ -MAS NMR spectra were recorded on a *Bruker*  
117 *ASX 100* spectrometer operating at 40.48 MHz  
118 (2.34 T). The pulse length was 1.3  $\mu\text{s}$  ( $\pi/4$ ) and 120 s delay  
119 time was used. The spinning rate was 12 kHz. The  $^{31}\text{P}$   
120 spectra were fitted to Gaussian-type functions, in  
121 accordance with the chemical shift distribution of the  
122 amorphous state. All NMR vertical scales in this paper  
123 are signal amplitude, normalized to the highest peak.

124  $^{207}\text{Pb}$  NMR spectra were obtained on a *Bruker ASX*  
125 *400* spectrometer. The large electronic shield around the  
126 lead nuclei results in a large chemical shift anisotropy  
127 (CSA). Hence, the free induction decays have to be re-  
128 corded from echoes measured at two frequency offsets.  
129 Then, two echoes are summed to obtain the whole spec-  
130 trum. This method, called VOCS (variable offsets cumu-  
131 lative spectrum) was developed for nuclei with large  
132 CSA [19]. The  $^{207}\text{Pb}$  frequency is 83.69 MHz at 9.4 T.  
133 Static echoes were obtained with a  $[\pi/2 - \tau - \pi]$  pulse  
134 sequence, with  $\pi/2 = 3 \mu\text{s}$  and  $\tau = 30 \mu\text{s}$ . The delay time  
135 was 30 s, sufficient to avoid signal saturation, and the

136 number of scans was 240. A 0.5M  $\text{Pb}(\text{NO}_3)_2$  solution  
 137 was used as a secondary reference for  $^{207}\text{Pb}$   
 138 ( $\delta = -2941$  ppm vs.  $\text{Pb}(\text{CH}_3)_4$  at 0 ppm).

139 The density of the glasses was measured by helium  
 140 pycnometry in a *Quantachrome Corp.* multipycnometer  
 141 by using bulk samples.

142 The thermal expansion coefficients, glass transition  
 143 temperatures and dilatometric softening points were  
 144 determined from thermal expansion curves obtained in  
 145 air with a *Netzsch Gerätebau* dilatometer, model 402  
 146 EP, at a heating rate of  $2\text{K min}^{-1}$ . Prismatic samples  
 147 of around 10mm in length were used for measurements.

### 148 3. Results

#### 149 3.1. Raman spectroscopy

150 The Raman spectra of  $(25 - x/2)\text{Li}_2\text{O} \cdot (25 - x/2)$   
 151  $\text{Na}_2\text{O} \cdot x\text{PbO} \cdot 50\text{P}_2\text{O}_5$  glass compositions are given  
 152 in Fig. 1 for  $x = 0, 10, 25, 40$  and  $50$  mol%. The spectrum  
 153 of the lead-free glass ( $x = 0$ ) shows three main peaks cor-  
 154 responding to the vibration modes of the  $\text{Q}^2$ -type  $\text{PO}_4$   
 155 tetrahedra: the asymmetric stretching mode of the  
 156 non-bridging oxygens,  $\nu_{\text{as}}(\text{PO}_2)$ , at  $\sim 1250\text{cm}^{-1}$ , the  
 157 symmetric stretching mode of the non-bridging oxygens,  
 158  $\nu_{\text{s}}(\text{PO}_2)$ , at  $\sim 1165\text{cm}^{-1}$ , and the symmetric stretching  
 159 mode of the P–O–P bonds,  $\nu_{\text{s}}(\text{POP})$ , at  $\sim 690\text{cm}^{-1}$ . In  
 160 addition, a weak contribution appears at  $\sim 1090\text{cm}^{-1}$   
 161 which is assigned to the symmetric stretching mode of

the non-bridging oxygens in  $\text{Q}^1$ -type  $\text{PO}_4$  terminal tetra- 162  
 hedra,  $\nu_{\text{s}}(\text{PO}_3^{2-})$  [26–29]. 163

Progressive addition of  $\text{PbO}$  to the phosphate glass 164  
 composition induces essentially in the Raman spectra 165  
 a shift towards lower wave numbers of the  $\nu_{\text{as}}(\text{PO}_2)$ , 166  
 $\nu_{\text{s}}(\text{PO}_2)$  and  $\nu_{\text{s}}(\text{PO}_3^{2-})$  mode stretching vibrations, 167  
 whereas the  $\nu_{\text{s}}(\text{POP})$  peak remains at approximately 168  
 the same Raman shift. 169

#### 3.2. $^{31}\text{P}$ -MAS NMR 170

The  $^{31}\text{P}$ -MAS NMR spectra are gathered in Fig. 2. 171  
 The spectrum of the 10 mol%  $\text{PbO}$  composition shows 172  
 a main resonance centered on  $-22.0$  ppm, which is 173  
 attributed to  $\text{Q}^2$ -type sites according to results obtained 174  
 by Sato et al. in alkali metaphosphate glasses [30]. An 175  
 additional weak resonance band centered at  $-8.8$  ppm 176  
 is assigned to a small amount of  $\text{Q}^1$ -type sites (or pyro- 177  
 phosphate groups), in accordance with Brow et al. [31]. 178  
 The presence of such groups is attributed to a small ex- 179  
 cess of cations compared to a metaphosphate composi- 180  
 tion. Higher  $\text{PbO}$  contents result in a shift of the 181  
 resonance frequencies of both  $\text{Q}^2$ - and  $\text{Q}^1$ -type sites to- 182  
 wards more negative  $\delta$  values, which is due to an in- 183  
 creased shielding effect of the  $\text{Pb}^{2+}$  cations. 184

#### 3.3. $^{207}\text{Pb}$ NMR 185

$^{207}\text{Pb}$  VOCS NMR spectra are shown in Fig. 3. The 186  
 resonance corresponding to 10 mol%  $\text{PbO}$  is centered 187  
 approximately on  $-2800$  ppm. As the  $\text{PbO}$  content in- 188  
 creases, the frequency value for the highest intensity is 189  
 shifted towards higher  $\delta$  values. As reported in binary 190  
 lead phosphate glasses, and stated in our previous paper 191  
 dealing with alkali lead oxynitride phosphate glasses 192  
 containing 25 mol%  $\text{PbO}$  [21], the observed  $\delta$  values 193  
 and resonance width correspond to typical chemical 194

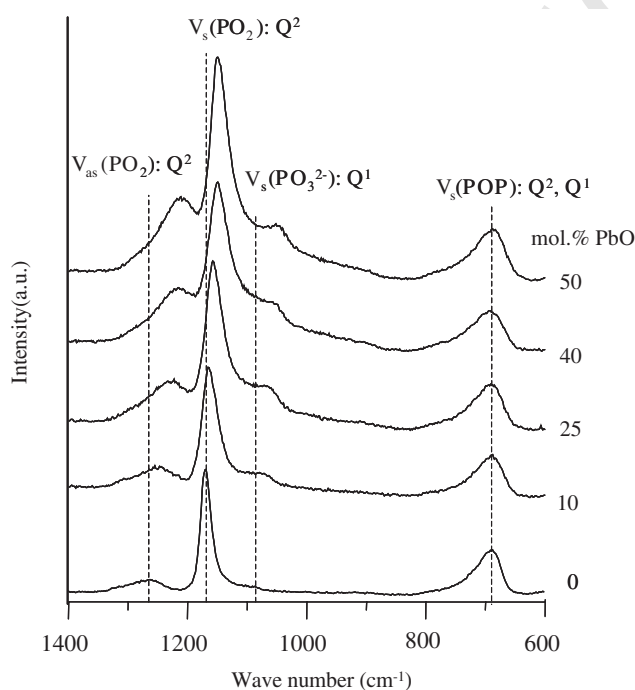


Fig. 1. Raman spectra of  $(25 - x/2)\text{Li}_2\text{O} \cdot (25 - x/2)\text{Na}_2\text{O} \cdot x\text{PbO} \cdot 50\text{P}_2\text{O}_5$  glasses for  $0 \leq x \leq 50$  mol%  $\text{PbO}$ .

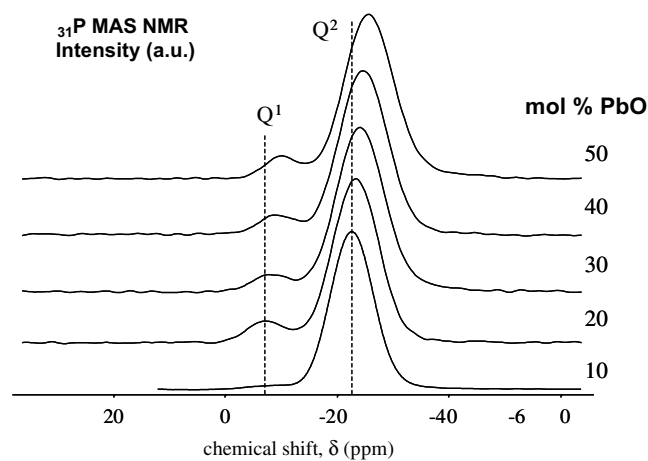


Fig. 2.  $^{31}\text{P}$ -MAS NMR spectra of  $(25 - x/2)\text{Li}_2\text{O} \cdot (25 - x/2)\text{Na}_2\text{O} \cdot x\text{PbO} \cdot 50\text{P}_2\text{O}_5$  glasses for  $10 \leq x \leq 50$  mol%  $\text{PbO}$ .

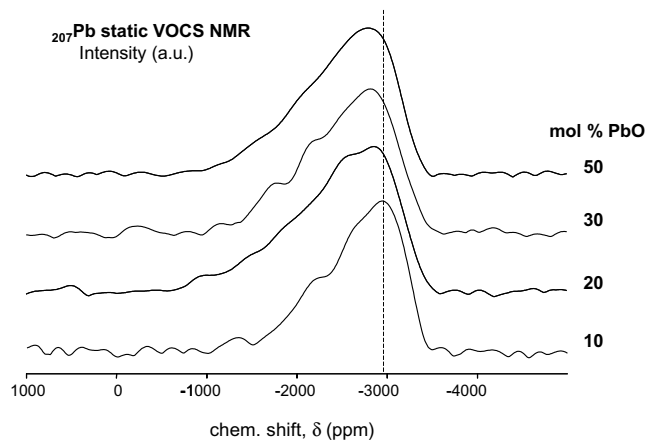


Fig. 3.  $^{207}\text{Pb}$ -VOCS NMR spectra of  $(25 - x/2)\text{Li}_2\text{O} \cdot (25 - x/2)\text{Na}_2\text{O} \cdot x\text{PbO} \cdot 50\text{P}_2\text{O}_5$  glasses for  $10 \leq x \leq 50$  mol% PbO.

195 shifts of lead cations with a high coordination number,  
 196 between 7 and 12, and to Pb–O bonds with a predomi-  
 197 nant ionic character [32]. From X-ray and neutron dif-  
 198 fraction results, Hoppe et al. [33,34] also concluded to  
 199 a large oxygen coordination polyhedron around  $\text{Pb}^{2+}$   
 200 in lead-containing phosphate glasses.

#### 201 3.4. Density and thermal properties

202 In Table 2 are gathered the densities, glass transition  
 203 and dilatometric softening temperatures, as well as the  
 204 thermal expansion coefficients determined within the  
 205 30–200 °C temperature range.

## 206 4. Discussion

### 207 4.1. Structural characterization

208 The Raman spectra of the  $(25 - x/2)\text{Li}_2\text{O} \cdot (25 - x/2)$   
 209  $\text{Na}_2\text{O} \cdot x\text{PbO} \cdot 50\text{P}_2\text{O}_5$  glass compositions (Fig. 1)  
 210 show, as the most important change, a shift towards  
 211 lower frequencies of  $\nu_{\text{as}}(\text{PO}_2)$ ,  $\nu_{\text{s}}(\text{PO}_2)$  and  $\nu_{\text{s}}(\text{PO}_3^{2-})$   
 212 when the PbO content increases. This is attributed to a

Table 2

Density values, glass transition temperatures ( $T_g$ ), dilatometric softening temperatures ( $T_s$ ) and coefficients of thermal expansion (CTE) of  $(25 - x/2)\text{Li}_2\text{O} \cdot (25 - x/2)\text{Na}_2\text{O} \cdot x\text{PbO} \cdot 50\text{P}_2\text{O}_5$  glasses

Mol% PbO	Density ( $\text{g cm}^{-3}$ ) ( $\pm 0.1 \text{ g cm}^{-3}$ )	$T_g$ (°C) ( $\pm 1$ °C)	$T_s$ (°C) ( $\pm 1$ °C)	CTE ( $\times 10^6 \text{ K}^{-1}$ ) <sub>30–200 °C</sub>
0	2.5	228	237	20
10	3.0	229	248	22
20	3.4	245	263	20
25	3.7	256	278	18
30	3.9	262	281	19
40	4.3	276	297	17
50	4.9	315	335	16

weakening of the P–O bonds which involve oxygen  
 atoms coordinating  $\text{Pb}^{2+}$  cations. On the other hand,  
 there is no shift of  $\nu_{\text{s}}(\text{POP})$ , so it can be concluded that  
 bridging oxygens of the  $\text{PO}_4$  tetrahedra are not directly  
 influenced by lead. In addition, it seems that an increase  
 in intensity of  $\nu_{\text{s}}(\text{PO}_3^{2-})$  takes place. This fact would  
 mean that the deviation from the metaphosphate com-  
 position is more important as the PbO content increases,  
 that is, however, not reflected on the chemical analysis  
 results given in Table 1.

In the  $^{31}\text{P}$ -MAS NMR spectra (Fig. 2), the shift to-  
 wards lower resonance frequencies of both  $\text{Q}^2$  and  $\text{Q}^1$   
 contributions which is observed when the PbO content  
 increases is explained by a greater shielding effect of  
 $\text{Pb}^{2+}$  cations on the phosphorus atoms: the greater the  
 IFS of the modifier cations, the greater the shielding  
 effect.

Fig. 4 shows the variation of the isotropic chemical  
 shift of the  $\text{Q}^2$ -type resonance band as a function of  
 the PbO content. The  $\delta(^{31}\text{P})$  value for the lead-free glass  
 composition has been taken from [22]. The linear rela-  
 tion found indicates an average bonding of the lead cat-  
 ions with all the non-bridging oxygen atoms of the  $\text{Q}^2$   
 (and  $\text{Q}^1$ ) groups, and also that the phosphorus atoms  
 of the  $\text{Q}^2$  (and  $\text{Q}^1$ ) groups have an average shielding  
 by the alkali metal and lead cations.

As can be seen in Fig. 3, an increase in PbO content  
 results in higher chemical shift values of the  $^{207}\text{Pb}$  reso-  
 nance bands. This is interpreted by a lowering of the  
 $\text{Pb}^{2+}$  coordination number and an increasing covalent  
 character of the Pb–O bonds. In other words, this corre-  
 sponds to a progressively greater former character of  
 lead, which is purely modifier at low PbO contents. Such  
 a phenomenon has been previously observed in the cor-  
 responding ‘LiNaPbPON’ oxynitride glass series con-  
 taining 25 mol% PbO, when the nitrogen content

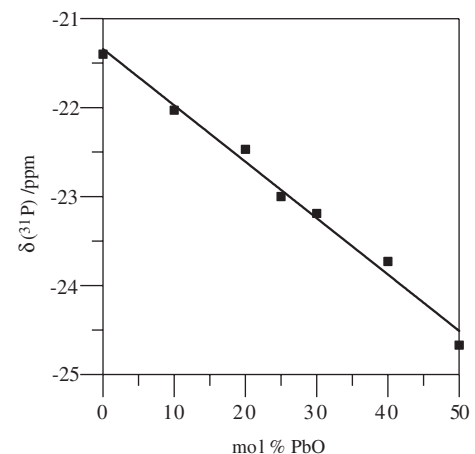


Fig. 4. Chemical shift of the  $^{31}\text{P}$  NMR  $\text{Q}^2$ -type resonance in  $(25 - x/2)\text{Li}_2\text{O} \cdot (25 - x/2)\text{Na}_2\text{O} \cdot x\text{PbO} \cdot 50\text{P}_2\text{O}_5$  glasses as a function of the PbO content. Line is drawn as a guide for the eyes.

249 increases [21]. So, increasing lead or substituting nitro-  
 250 gen for oxygen in  $\text{Li}_2\text{O}-\text{Na}_2\text{O}-\text{PbO}-\text{P}_2\text{O}_5$  metaphos-  
 251 phate glass compositions seems to produce a similar  
 252 effect on the coordination sphere of the  $\text{Pb}^{2+}$  cations,  
 253 which, in both cases, is formed exclusively by oxygen  
 254 [21]. The phenomenon is much more manifest in ‘LiN-  
 255 aPbPON’ oxynitride glasses, that demonstrates the par-  
 256 ticular role of nitrogen. In fact, the N/O substitution  
 257 decreases directly the number of non-bridging oxygens  
 258 available for the coordination of lead atoms. In the case  
 259 of ‘LiNaPbPO’ oxide glasses, as lead substitutes for al-  
 260 kali cations, the decrease in available non-bridging oxy-  
 261 gens only results from the higher number of oxygens  
 262 required by  $\text{Pb}^{2+}$  compared to  $\text{Li}^+$  or  $\text{Na}^+$ . As more lead  
 263 is added, this number is progressively reduced.

#### 264 4.2. Influence of the PbO content on the molar volume. 265 Thermal properties

266 In Fig. 5, the density values ( $\rho$ ) and PbO molar vol-  
 267 umes ( $V_m$ ) for the different  $(25 - x/2)\text{Li}_2\text{O} \cdot (25 - x/2)$   
 268  $\text{Na}_2\text{O} \cdot x\text{PbO} \cdot 50\text{P}_2\text{O}_5$  glasses have been plotted as a  
 269 function of the PbO content  $x$ . For each composition  
 270 the PbO molar volume is calculated using the following  
 271 equation:

$$273 V_m(\text{PbO}) = (x_i \cdot M) / \rho, \quad (1)$$

274 where  $\rho$ ,  $x_i$  and  $M$  are the density, the PbO molar frac-  
 275 tion in the glass composition and the molar weight of  
 276 PbO, respectively.

277 While the density increases linearly with  $x$  (because it  
 278 is an additive property), the PbO molar volume does not  
 279 follow the linear increase simulated by the dashed line in  
 280 Fig. 5. It increases along the whole composition range,  
 281 however it deviates all the more as higher is the PbO  
 282 content. Therefore, an increasing lead content results  
 283 in a decrease in the volume occupied by the coordination  
 284 sphere of each  $\text{Pb}^{2+}$  cation. This is in accordance with  
 285 the  $^{207}\text{Pb}$  NMR results.

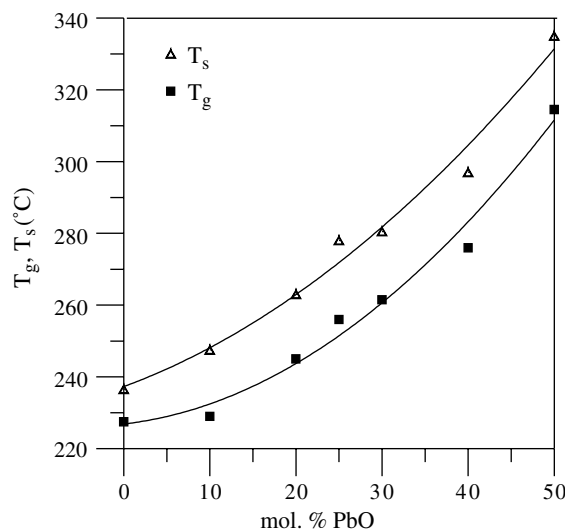


Fig. 6. Glass transition temperature ( $T_g$ ) and dilatometric softening temperature ( $T_s$ ) of  $(25 - x/2)\text{Li}_2\text{O} \cdot (25 - x/2)\text{Na}_2\text{O} \cdot x\text{PbO} \cdot 50\text{P}_2\text{O}_5$  glasses as a function of the PbO content. Lines are drawn as a guide for the eyes.

286 In Figs. 6 and 7 are shown the variations of  $T_g$  and  
 287  $T_s$ , and CTE, respectively, as a function of the PbO con-  
 288 tent. In all cases a non-linear variation can be observed,  
 289 which is more significant from 20 to 25 mol% PbO.  $T_g$   
 290 and  $T_s$  similarly increase while CTE decreases. Such a  
 291 behavior can be explained through two factors. On  
 292 one hand, the influence of the mixed alkali effect  
 293 (MAE) results in lower  $T_g$  and  $T_s$ , and in higher CTE  
 294 than those of single alkali compositions. It is greater  
 295 at high alkali content [35,36]. On the other hand, PbO  
 296 increases the covalent character of the glass network,  
 297 that leads to higher  $T_g$  and  $T_s$ , and lower CTE values.  
 298 This effect is more important between 25 and 50 mol%  
 299 of PbO than at lower lead contents, as indicated by  
 300 the non-linear behavior of the PbO molar volume. The  
 301 smaller increase in the molar volume at high PbO con-

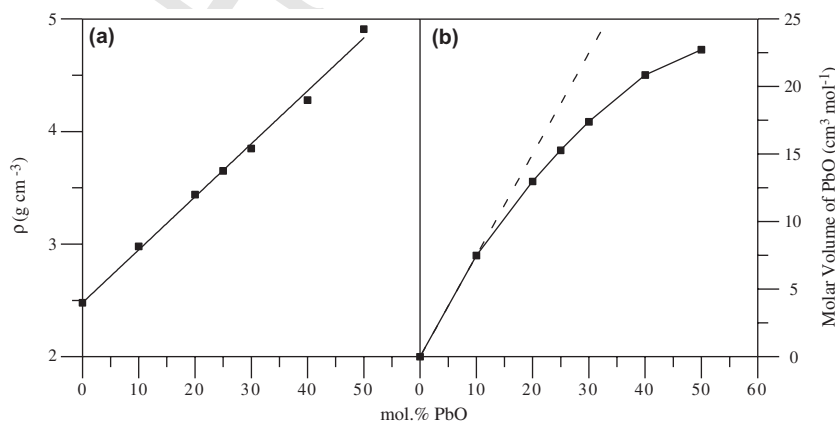


Fig. 5. Density (a) and PbO molar volume (b) variations as a function of the PbO content in  $(25 - x/2)\text{Li}_2\text{O} \cdot (25 - x/2)\text{Na}_2\text{O} \cdot x\text{PbO} \cdot 50\text{P}_2\text{O}_5$  glasses. The dashed line in (b) is only drawn as a reference for comparison with the experimental values.

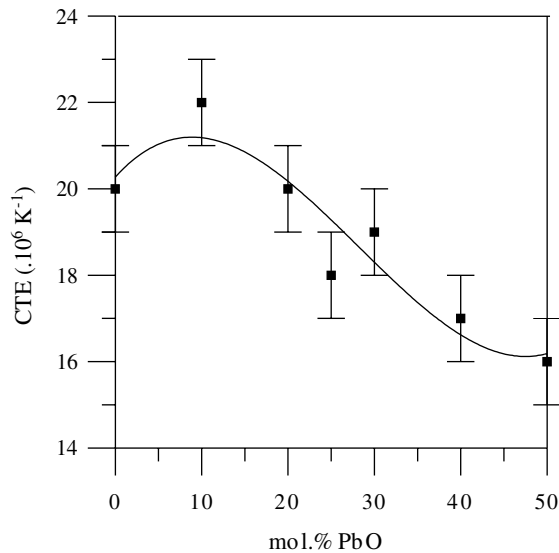


Fig. 7. Coefficient of thermal expansion (CTE) of  $(25 - x/2)\text{Li}_2\text{O} \cdot (25 - x/2)\text{Na}_2\text{O} \cdot x\text{PbO} \cdot 50\text{P}_2\text{O}_5$  glasses as a function of the PbO content. Line is drawn as a guide for the eyes.

302 tents gives rise to a larger increase in the characteristic  
303 temperatures and a more pronounced decrease in CTE.

### 304 5. Conclusions

305 Raman spectroscopy,  $^{31}\text{P}$ -MAS and  $^{207}\text{Pb}$ -VOCS  
306 NMR of  $(25 - x/2)\text{Li}_2\text{O} \cdot (25 - x/2)\text{Na}_2\text{O} \cdot x\text{PbO} \cdot$   
307  $50\text{P}_2\text{O}_5$  glass compositions ( $0 \leq x \leq 50$  mol%) have  
308 shown that the  $\text{Pb}^{2+}$  coordination sphere is large, with  
309 coordination numbers about 7–12. An increase in the  
310 PbO proportion induces a weakening of P–O bonds of  
311 the  $\text{PO}_4$  tetrahedra involving the non-bridging oxygens  
312 coordinating  $\text{Pb}^{2+}$ . It results, in addition, in more covalent  
313 Pb–O bonds and a lower coordination number of  
314 lead.

315 The variation versus lead content of the PbO molar  
316 volume, the glass transition and dilatometric softening  
317 temperatures, and the thermal expansion coefficient is  
318 consistent with the modification of the lead local envi-  
319 ronment, and the progressive attenuation of the mixed  
320 alkali effect.

### 321 Acknowledgment

322 This work has been sponsored by the CICYT of  
323 Spain through the project MAT (2000-0952-C02-01)  
324 and by an Integrated Action CSIC-CNRS (HF2001-  
325 124).

### References

- [1] N.H. Ray, C.J. Lewis, J.N.C. Laycock, W.D. Robinson, *Glass Technol.* 14 (2) (1973) 50. 327  
328
- [2] N.H. Ray, J.N.C. Laycock, W.D. Robinson, *Glass Technol.* 14 (2) (1973) 55. 329  
330
- [3] Y.B. Peng, D.E. Day, *Glass Technol.* 32 (1991) 166. 331
- [4] Y.B. Peng, D.E. Day, *Glass Technol.* 32 (6) (1991) 200. 332
- [5] Y. He, D.E. Day, *Glass Technol.* 33 (6) (1992) 214. 333
- [6] I.W. Donald, *J. Mater. Sci.* 28 (1993) 2841. 334
- [7] D.E. Day, *Proc. XIX Int. Congr. Glass* 2 (2001) 17. 335
- [8] I.W. Donald, B.L. Metcalfé, R.N.J. Taylor, *J. Mater. Sci.* 32 (1997) 5851. 336  
337
- [9] S. Jiang, M. Myers, N. Peyghambarian, *J. Non-Cryst. Solids* 239 (1998) 143. 338  
339
- [10] M.N. Khan, R. Harani, M.M. Ahmed, C.A. Hogarth, *J. Mater. Sci.* 20 (1985) 2207. 340  
341
- [11] S. Dai, A. Sugiyama, L. Hu, Z. Liu, G. Huang, Z. Jiang, *J. Non-Cryst. Solids* 311 (2002) 138. 342  
343
- [12] F. Chen, X.-L. Wang, X.-S. Li, L.-L. Hu, Q.-M. Lu, K.-M. Wang, B.-R. Shi, D.-Y. Shen, *Appl. Surf. Sci.* 193 (2002) 92. 344  
345
- [13] R.K. Brow, M.R. Reidmeyer, D.E. Day, *J. Non-Cryst. Solids* 99 (1988) 178. 346  
347
- [14] B.C. Bunker, D.R. Tallant, C.A. Balfe, R.J. Kirkpatrick, G.L. Turner, M.R. Reidmeyer, *J. Amer. Ceram. Soc.* 70 (9) (1987) 675. 348  
349
- [15] M.R. Reidmeyer, M. Rajaram, D.E. Day, *J. Non-Cryst. Solids* 85 (1986) 186. 350  
351
- [16] R.W. Larson, D.E. Day, *J. Non-Cryst. Solids* 88 (1986) 97. 352
- [17] F. Muñoz, L. Pascual, A. Durán, R. Marchand, *Phys. Chem. Glasses* 43C (2002) 113. 353  
354
- [18] F. Fayon, PhD thesis, University of Orléans, France, 1998. 355
- [19] F. Fayon, C. Landron, K. Sakurai, C. Bessada, D. Massiot, *J. Non-Cryst. Solids* 243 (1999) 39. 356  
357
- [20] U. Hoppe, *J. Non-Cryst. Solids* 183 (1995) 85. 358
- [21] F. Muñoz, L. Pascual, A. Durán, L. Montagne, G. Palavit, R. Berjoan, R. Marchand, *J. Non-Cryst. Solids* 324 (2003) 142. 359  
360
- [22] A. Le Sauze, L. Montagne, G. Palavit, F. Fayon, R. Marchand, *J. Non-Cryst. Solids* 263&264 (2000) 139. 361  
362
- [23] U. Hoppe, R. Kranold, A. Ghosh, C. Landron, J. Neufeind, P. Jóvári, *J. Non-Cryst. Solids* 293–295 (2001) 158. 363  
364
- [24] M. Abid, M. Et-tabirou, M. Taibi, *Mater. Sci. Eng. B* 97 (2002) 20. 365  
366
- [25] H.S. Liu, T.S. Chinand, S.W. Yung, *Mater. Chem. Phys.* 50 (1997) 1. 367  
368
- [26] A. Mekki, G.D. Khattak, L.E. Wenger, *J. Non-Cryst. Solids* 330 (2003) 156. 369  
370
- [27] K. Meyer, *J. Non-Cryst. Solids* 209 (1997) 227. 371
- [28] J. Koo, B.-S. Bae, H.-K. Na, *J. Non-Cryst. Solids* 212 (1997) 173. 372
- [29] J.J. Hudgens, R.K. Brow, D.R. Tallant, S.W. Martin, *J. Non-Cryst. Solids* 223 (1998) 21. 373  
374
- [30] R.K. Sato, R.J. Kirkpatrick, R.K. Brow, *J. Non-Cryst. Solids* 143 (1992) 257. 375  
376
- [31] R.K. Brow, R.J. Kirkpatrick, G.L. Turner, *J. Non-Cryst. Solids* 116 (1990) 39. 377  
378
- [32] F. Fayon, I. Farnan, C. Bessada, D. Massiot, J.P. Coutures, *J. Amer. Chem. Soc.* 119 (1997) 6837. 379  
380
- [33] U. Hoppe, G. Walter, R. Kranold, D. Stachel, *J. Non-Cryst. Solids* 263&264 (2000) 29. 381  
382
- [34] U. Hoppe, R. Kranold, A. Ghosh, C. Landron, J. Neufeind, P. Jóvári, *J. Non-Cryst. Solids* 328 (2003) 146. 383  
384
- [35] J.M.F. Navarro, in: *El Vidrio*, Consejo Superior de Investigaciones Científicas, Madrid, Spain, 1991. 385  
386
- [36] W. Vogel, *Glass Chemistry*, 2nd Ed., Springer, Berlin, 1985. 387  
388